

# Passivity-based Control for 2DOF Robot Manipulators with Antagonistic Bi-articular Muscles

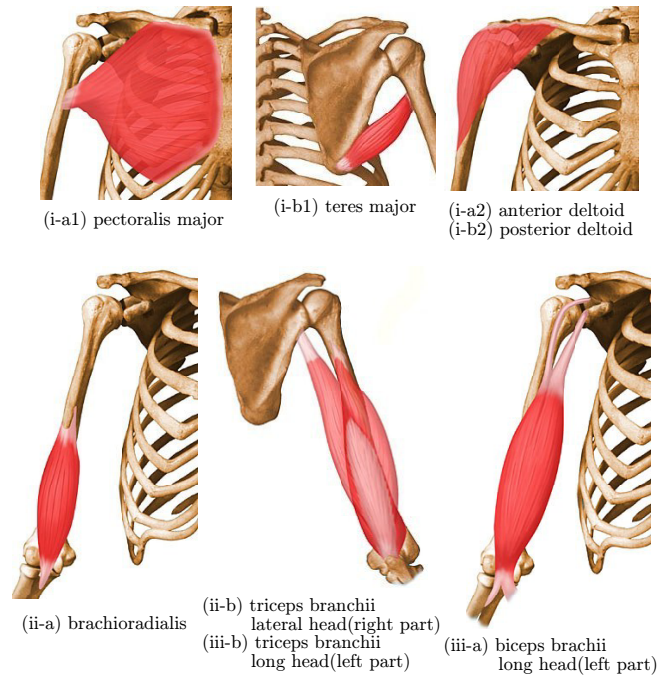
Hiroyuki Kawai, Toshiyuki Mura, Ryuichi Sato and Masayuki Fujita

**Abstract**—This paper investigates a passivity-based control for two degree of freedom(2DOF) robot manipulators with antagonistic bi-articular muscles which are passing over adjacent two joints and acting the both joints simultaneously. The manipulator dynamics of three muscle torques, we call the bi-articular manipulator dynamics, is constructed in order to design the control input. Stability analysis with respect to our proposed control law is discussed by using the important property which is concerned with the passivity, although the passivity of the bi-articular manipulator dynamics can not be shown on account of antagonistic bi-articular muscles explicitly. Finally, simulation results are shown in order to confirm the proposed method.

## I. INTRODUCTION

Modern robots are expected to safely and dependably co-habitat with humans in homes and workplaces, providing support in services, healthcare, assistance and so on [1]. When mechanical systems are working under dynamical environments, sensory information is needed to behave autonomously. The authors have proposed a vision based control [2] and vision and force based control [3] in order to control the motion of the rigid robot manipulators in an efficient manner. Although rigid robot manipulators can move with high torque and high speed, these would not be suitable as modern robots which interact human motion, i.e. rehabilitation, human support, surgery and so on.

On the other hand, human motion involves neurons, muscles, chemical reactions, bones, joints, and ligaments. Recently, analysis of human motion and robot motion control by using the mechanism of the human body increasingly gains attention. For example, the configuration of the affected human limb(s) can be controlled at each joint by using rehabilitation robots, so that missing motor synergies can now be compensated for severely disabled patients [4]. M. Kuschel *et al.* [5] have proposed a mathematical model for visual-haptic perception of compliant objects based on psychophysical experiments. Wang *et al.* [6] dealt with a neural network based inverse optimal neuromuscular electrical simulation controller to enable the lower limb to track a desired trajectory. Antagonistic bi-articular muscles, which are passing over adjacent two joints and acting the both joints simultaneously as shown in Fig. 1, are known as one of



Copyright 2003-2004 University of Washington. All rights reserved including all photographs and images. No re-use, re-distribution or commercial use without prior written permission of the authors and the University of Washington.

Fig. 1. Muscles of Arm. (i)Antagonistic mono-articular muscles attached to the shoulder joint consist of two flexor muscles, i.e., pectoralis major and anterior deltoid, and two extensor muscles, i.e., teres major and posterior deltoid. (ii)Antagonistic mono-articular muscles attached to the elbow joint consist of brachioradialis and triceps brachii lateral head. (iii)Antagonistic bi-articular muscles attached to both the shoulder and the elbow joint consist of biceps brachii long head and triceps brachii long head.

most important mechanisms of the human body associated with motion. Kumamoto *et al* give us the effects of the existence of antagonistic bi-articular muscles [7]–[9]. Oh and Hori [10] have proposed two-degree-of-freedom control for robot manipulator with antagonistic bi-articular muscles. However, stability analysis is not discussed in these works explicitly.

This paper deals with a passivity-based control for two degree of freedom(2DOF) robot manipulators with antagonistic bi-articular muscles. Control objectives are both a regulation and a trajectory tracking like a standard robot motion control. Stability analysis with respect to our proposed control law is discussed by using the important property which is concerned with the passivity. This is one of main contributions of this research. The simulation results show the validity of the proposed method.

H. Kawai is with Department of Robotics, Kanazawa Institute of Technology, Ishikawa 921-8501, Japan [hiroyuki@neptune.kanazawa-it.ac.jp](mailto:hiroyuki@neptune.kanazawa-it.ac.jp)

T. Mura is with Master Program of Innovation for Design and Engineering Advanced Institute of Industrial Technology, Tokyo 140-0011, Japan

R. Sato is with Department of Robotics, Kanazawa Institute of Technology, Ishikawa 921-8501, Japan

M. Fujita is with Department of Mechanical and Control Engineering, Tokyo Institute of Technology, Tokyo 152-8550, Japan

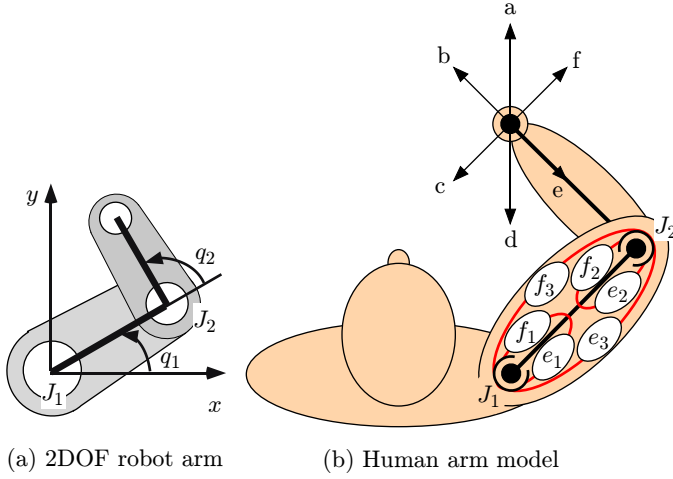


Fig. 2. (a) 2DOF robot arm. (b) Human arm model. Two couples of the antagonistic mono-articular muscles of  $f_1$  and  $e_1$ , and of  $f_2$  and  $e_2$  are attached to the joints of  $J_1$  and  $J_2$ , respectively. A couple of the antagonistic bi-articular muscles  $f_3$  and  $e_3$  are attached to both joints of  $J_1$  and  $J_2$ .

## II. MODEL OF 2DOF ROBOT MANIPULATORS WITH ANTAGONISTIC BI-ARTICULAR MUSCLES

### A. Antagonistic Bi-articular Muscle Torque

The dynamics of  $n$ -link rigid robot manipulators can be written as

$$M(q)\ddot{q} + C(q, \dot{q})\dot{q} + g(q) = T \quad (1)$$

where  $q$ ,  $\dot{q}$  and  $\ddot{q}$  are the joint angle, velocity and acceleration, respectively.  $T$  is the vector of the input torque.  $M(q) \in \mathcal{R}^{n \times n}$  is the manipulator inertia matrix,  $C(q, \dot{q}) \in \mathcal{R}^{n \times n}$  is the Coriolis matrix and  $g(q) \in \mathcal{R}^n$  is the gravity vector [11]. In the case of 2DOF robot manipulator as shown in Fig. 2(a), the dynamics can be concretely represented as

$$\begin{bmatrix} M_1 + 2M_2 + 2RC_2 & 2M_2 + RC_2 \\ 2M_2 + RC_2 & 2M_2 \end{bmatrix} \begin{bmatrix} \ddot{q}_1 \\ \ddot{q}_2 \end{bmatrix} + \begin{bmatrix} -RS_2\dot{q}_2 & -RS_2(\dot{q}_1 + \dot{q}_2) \\ RS_2\dot{q}_1 & 0 \end{bmatrix} \begin{bmatrix} \dot{q}_1 \\ \dot{q}_2 \end{bmatrix} + \begin{bmatrix} g(m_1l_{g1} + m_2l_2)C_1 + g(m_2l_{g2})C_{12} \\ g(m_2l_{g2})C_{12} \end{bmatrix} = \begin{bmatrix} T_1 \\ T_2 \end{bmatrix} \quad (2)$$

where  $M_1 = m_1l_{g1}^2 + m_2l_1^2 + \tilde{I}_1$ ,  $M_2 = \frac{1}{2}(m_2l_{g2}^2 + \tilde{I}_2)$  and  $R = m_2l_1l_{g2}$ .  $m_i$  and  $l_i$  are the weight and the length of the link  $i$ ,  $l_{gi}$  is the distance from the center of a joint  $i$  to the center of the gravity point of the link  $i$ ,  $\tilde{I}_i$  is the moment of inertia about an axis through the center of mass of link  $i$  ( $i = 1, 2$ ).  $S_i$ ,  $C_i$ ,  $S_{ij}$  and  $C_{ij}$  mean  $\sin q_i$ ,  $\cos q_i$ ,  $\sin(q_i + q_j)$  and  $\cos(q_i + q_j)$ , respectively.

While a real human arm has four pairs of antagonistic muscles as shown in Fig. 1, human arm model can be simplified as three pairs of antagonistic muscles as depicted in Fig. 2(b) [8]. Generally, the joint torque  $T$  will be designed as a control input directly in robot motion control. Because a couple of bi-articular muscles are attached to both joints

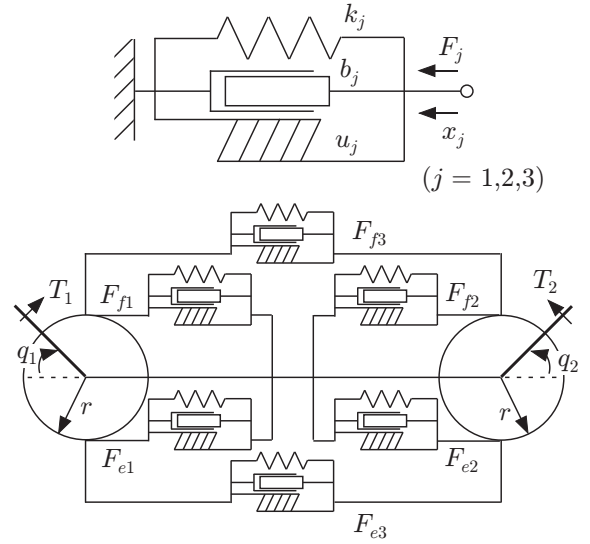


Fig. 3. Visco-elastic muscle model [8].  $F_j$ : output force,  $u_j$ : contractile force,  $k_j$ : elastic coefficient,  $b_j$ : coefficient of viscosity,  $x_j$ : contracting length.

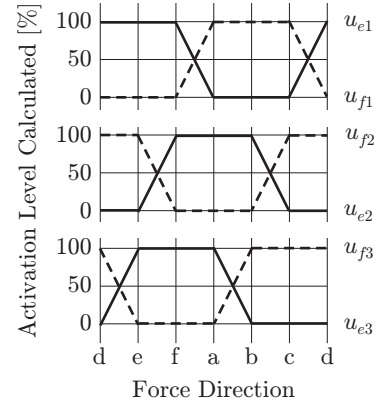


Fig. 4. Each muscle respond depending on the direction of the force at the tip point [8].

as shown in Fig. 3, the joint torques are described as

$$\begin{aligned} T_i &= (F_{fi} - F_{ei})r + (F_{f3} - F_{e3})r \\ &= (u_{fi} - u_{ei})r - (u_{fi} + u_{ei})k_i r^2 q_i - (u_{fi} + u_{ei})b_i r^2 \dot{q}_i \\ &\quad + (u_{f3} - u_{e3})r - (u_{f3} + u_{e3})k_3 r^2 (q_1 + q_2) \\ &\quad - (u_{f3} + u_{e3})b_3 r^2 (\dot{q}_1 + \dot{q}_2) \quad (i = 1, 2) \end{aligned} \quad (3)$$

where  $F_{fj}$  and  $F_{ej}$  are forces generated by flexor muscle and by extensor muscle,  $u_{fj}$  and  $u_{ej}$  represent contractile forces of flexor muscle and of extensor muscle ( $j = 1, 2, 3$ ).  $r$ ,  $k_j$  and  $b_j$  are the radius of the joint pulley, elastic coefficients and visco coefficients, respectively [7].

Fig. 4 shows the activation levels of each muscle respond depending on the direction of the force at the tip point. a-f mean the direction of the force at the tip point in Fig. 2(b). From Fig. 4, the activation levels of the antagonistic pair muscles satisfy

$$u_{fj} + u_{ej} = 1 \quad (j = 1, 2, 3). \quad (4)$$

Using this important property with respect to the antagonistic pair muscles, the joint torques can be transformed into

$$T_i = (2u_{fi} - 1)r - k_i r^2 q_i - b_i r^2 \dot{q}_i + (2u_{f3} - 1)r - k_3 r^2 (q_1 + q_2) - b_3 r^2 (\dot{q}_1 + \dot{q}_2) \quad (i = 1, 2) \quad (5)$$

Here we assume that the contractile force of flexor muscle  $u_{fi}$  can be decided by an actuator. Then, the joint torques (5) are represented as

$$T_i = \tau_i + \tau_3 - k_i r^2 q_i - k_3 r^2 (q_1 + q_2) - b_i r^2 \dot{q}_i - b_3 r^2 (\dot{q}_1 + \dot{q}_2) \quad (i = 1, 2) \quad (6)$$

where muscle torques are defined as  $\tau_i := (2u_{fi} - 1)r$ . Therefore, we will design the bi-articular muscle torque  $\tau \in \mathcal{R}^3$  as the control input for the 2DOF robot manipulators with antagonistic bi-articular muscles.

### B. Dynamics of 2DOF Robot Manipulators with Antagonistic Bi-articular Muscles

In this subsection, we construct the manipulator dynamics of three muscle torques in order to design the control input. We now suggest that the dynamics of the antagonistic bi-articular muscles torque is defined as

$$\begin{aligned} \tau_3 &= \frac{1}{2}(m_2 l_{g2}^2 + \tilde{I}_2)(\ddot{q}_1 + \ddot{q}_2) + g(m_2 l_{g2})C_{12} \\ &\quad + k_3 r^2 (q_1 + q_2) + b_3 r^2 (\dot{q}_1 + \dot{q}_2) \\ &= M_2(\ddot{q}_1 + \ddot{q}_2) + g(m_2 l_{g2})C_{12} \\ &\quad + k_3 r^2 (q_1 + q_2) + b_3 r^2 (\dot{q}_1 + \dot{q}_2). \end{aligned} \quad (7)$$

From Eq. (2), the manipulator dynamics of three antagonistic muscles torques can be represented as

$$\begin{aligned} &\begin{bmatrix} M_1 + M_2 + 2RC_2 & M_2 + RC_2 & 0 \\ M_2 + RC_2 & M_2 & 0 \\ 0 & 0 & M_2 \end{bmatrix} \begin{bmatrix} \ddot{q}_1 \\ \ddot{q}_2 \\ \ddot{q}_1 + \ddot{q}_2 \end{bmatrix} \\ &+ \begin{bmatrix} -RS_2 \dot{q}_2 & -RS_2(\dot{q}_1 + \dot{q}_2) & 0 \\ RS_2 \dot{q}_1 & 0 & 0 \\ 0 & 0 & 0 \end{bmatrix} \begin{bmatrix} \dot{q}_1 \\ \dot{q}_2 \\ \dot{q}_1 + \dot{q}_2 \end{bmatrix} \\ &+ \begin{bmatrix} g(m_1 l_{g1} + m_2 l_2)C_1 \\ 0 \\ g(m_2 l_{g2})C_{12} \end{bmatrix} \\ &+ K_r \begin{bmatrix} q_1 \\ q_2 \\ q_1 + q_2 \end{bmatrix} + B_r \begin{bmatrix} \dot{q}_1 \\ \dot{q}_2 \\ \dot{q}_1 + \dot{q}_2 \end{bmatrix} = \begin{bmatrix} \tau_1 \\ \tau_2 \\ \tau_3 \end{bmatrix} \end{aligned} \quad (8)$$

where  $K_r := \text{diag}\{k_1, k_2, k_3\}r^2 \in \mathcal{R}^{3 \times 3}$  and  $B_r := \text{diag}\{b_1, b_2, b_3\}r^2 \in \mathcal{R}^{3 \times 3}$ . Moreover, we define the extended joint angle vector for the manipulator dynamics of three antagonistic muscles torques as

$$\theta = \begin{bmatrix} q_1 \\ q_2 \\ q_1 + q_2 \end{bmatrix}. \quad (9)$$

Based on the well-known form of the manipulator dynamics (1), the manipulator dynamics with antagonistic bi-articular

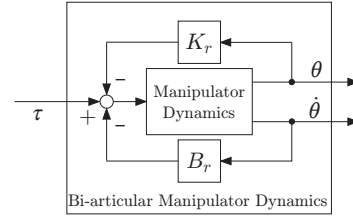


Fig. 5. Block diagram of the bi-articular manipulator dynamics.

muscles, we call the bi-articular manipulator dynamics, can be described as

$$M_b(\theta)\ddot{\theta} + C_b(\theta, \dot{\theta})\dot{\theta} + g_b(\theta) + K_r\theta + B_r\dot{\theta} = \tau \quad (10)$$

where the elements of  $M_b(\theta) \in \mathcal{R}^{3 \times 3}$ ,  $C_b(\theta, \dot{\theta}) \in \mathcal{R}^{3 \times 3}$  and  $g_b(\theta) \in \mathcal{R}^3$  are correspond to Eq. (8). The block diagram of the bi-articular manipulator dynamics is depicted in Fig. 5. Then the bi-articular manipulator dynamics has following important properties.

*Property 1:* The inertia matrix  $M_b(\theta)$  preserves the positive definiteness.

*Property 2:*  $\dot{M}_b(\theta) - 2C_b(\theta, \dot{\theta})$  is skew-symmetric.

*Remark 1:* The form of the manipulator dynamics with three muscle torques (8) is not constructed uniquely, since the degree of freedom for the control input  $\tau$  is greater than that for the joint  $q$ . For example, Oh and Hori [10] have proposed diagonalized inertia matrix in order to decouple the correlation of joint torques, although the positive definiteness of the inertia matrix is not preserved. Because Property 1 and 2 are very important factors for stability analysis, we construct the bi-articular manipulator dynamics (10) which satisfies them.

### III. PASSIVITY-BASED CONTROL LAW

The control objective of the manipulator with antagonistic bi-articular muscles is that both the joint angle and the joint velocity coincide with the desired ones, respectively. For the bi-articular manipulator dynamics, we propose the control law as

$$\tau = M_b(\theta)\dot{v} + C_b(\theta, \dot{\theta})v + g_b(\theta) - \dot{e} + K_r\theta_d + B_r\dot{\theta} \quad (11)$$

where  $v$ ,  $\dot{v}$ ,  $e$  and  $\dot{e}$  are defined as

$$\begin{aligned} v &= \dot{\theta}_d - K_r e, \quad \dot{v} = \ddot{\theta}_d - K_r \dot{e} \\ e &= \theta - \theta_d, \quad \dot{e} = \dot{\theta} - \dot{\theta}_d \end{aligned}$$

and  $\theta_d := [q_{d1} \ q_{d2} \ q_{d1} + q_{d2}]^T$  is a desired extended joint angle. Substituting Eq. (11) into Eq. (10), the closed-loop system can be obtained as

$$M_b(\theta)\dot{s} + C_b(\theta, \dot{\theta})s + s = 0 \quad (12)$$

where  $s := \dot{e} + K_r e$ . Here, we define the state of the closed-loop system with the bi-articular manipulator dynamics and the proposed control law as

$$x = \begin{bmatrix} e \\ \dot{e} \end{bmatrix}. \quad (13)$$

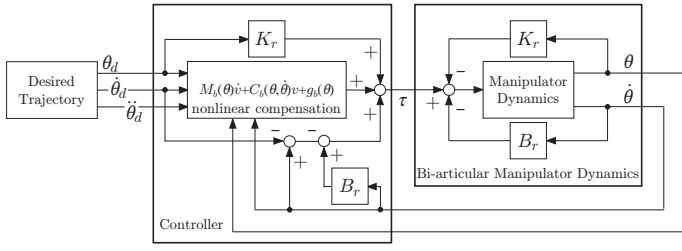


Fig. 6. Block diagram of the closed-loop system with the bi-articular manipulator dynamics and the proposed control law.

The block diagram of the closed-loop system is depicted in Fig. 6. It is noted that the equilibrium point  $x = 0$  is equal to  $e = 0$  and  $s = 0$ . If the equilibrium point  $x = 0$ , then the joint angle and the joint velocity coincide with the desired ones and the control objective is achieved. We show the following theorem concerning the stability of closed-loop system.

*Theorem 1:* The equilibrium point  $x = 0$  for the closed-loop system (12) is asymptotic stable.

*Proof:* Consider the following positive definite function

$$V = \frac{1}{2} s^T M_b(\theta) s + e^T K_r e. \quad (14)$$

The positive definiteness of the function  $V$  results from Property 1. Differentiating (14) with respect to time, we obtain

$$\begin{aligned} \dot{V} &= s^T \dot{M}_b(\theta) \dot{s} + \frac{1}{2} s^T \dot{M}_b(\theta) s + 2e^T K_r \dot{e} \\ &= s^T (-C_b(\theta, \dot{\theta}) s - s) + \frac{1}{2} s^T \dot{M}_b(\theta) s + 2e^T K_r \dot{e} \\ &= -s^T s + \frac{1}{2} s^T (\dot{M}_b(\theta) - 2C_b(\theta, \dot{\theta})) s + 2e^T K_r \dot{e} \end{aligned} \quad (15)$$

Using Property 2, i.e., the skew-symmetry of the matrix  $\dot{M}_b(\theta) - 2C_b(\theta, \dot{\theta})$  yields

$$\begin{aligned} \dot{V} &= -(\dot{e} + K_r e)^T (\dot{e} + K_r e) + 2e^T K_r \dot{e} \\ &= -\dot{e}^T \dot{e} - e^T K_r^2 e. \end{aligned} \quad (16)$$

From the positive definiteness of  $K_r$ , this completes the proof. ■

Stability analysis with respect to our proposed control law is discussed by using Property 1 and 2 which are concerned with the passivity, although the passivity of the bi-articular manipulator dynamics can not be shown on account of antagonistic bi-articular muscles explicitly. Indeed, our proposed control law is similar to one of passivity-based control laws for robot manipulator which is well-known as the Slotine and Li scheme [12]. This is one of main contributions of this research.

#### IV. SIMULATION RESULTS

In this section, we show the simulation results in order to confirm the proposed method. Moreover we give the possibility of a sensorless control for 2DOF robot manipulators with antagonistic bi-articular muscles. The parameters of the

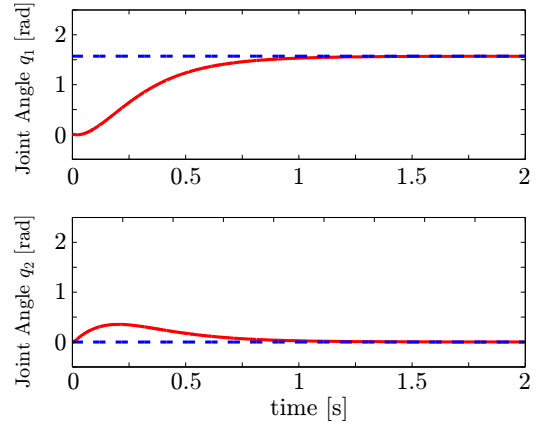


Fig. 7. Step response in the case of  $q_{d1} = \frac{\pi}{2}$ ,  $q_{d2} = 0$  (solid:Joint angles, dashed:Desired ones).

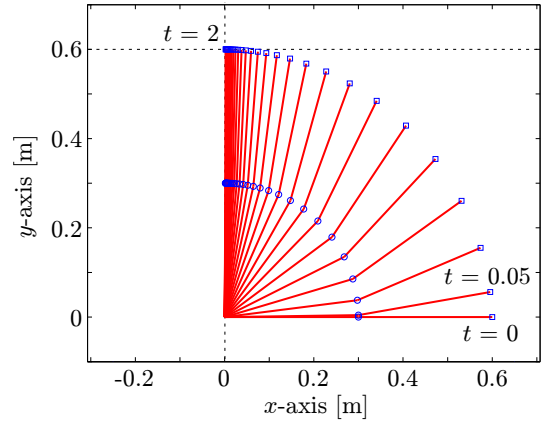


Fig. 8. Trajectory of the arm in the case of  $q_{d1} = \frac{\pi}{2}$ ,  $q_{d2} = 0$ .

bi-articular manipulator dynamics used in the simulation are  $m_1 = 1.75[\text{kg}]$ ,  $m_2 = 1.75[\text{kg}]$ ,  $l_1 = 0.3[\text{m}]$ ,  $l_2 = 0.3[\text{m}]$ ,  $l_{g1} = 0.15[\text{m}]$ ,  $l_{g2} = 0.15[\text{m}]$ ,  $\tilde{I}_1 = 0.014[\text{kg} \cdot \text{m}^2]$ ,  $\tilde{I}_2 = 0.014[\text{kg} \cdot \text{m}^2]$ ,  $r = 0.05[\text{m}]$  and  $b_1 = b_2 = b_3 = 400[\text{Ns/m}]$ , and the effect of the gravity is ignored. Because we guess that elastic coefficients depend on the strength of muscles, we select  $k_1 = 3,000[\text{N/m}]$ ,  $k_2 = 2,000[\text{N/m}]$  and  $k_3 = 4,000[\text{N/m}]$  based on Fig. 1.

We consider both set-point problems and trajectory tracking ones. In the cases of set-point problems, the initial angles are  $q_1(0) = 0[\text{rad}]$  and  $q_2(0) = 0[\text{rad}]$ . In the cases of trajectory tracking problems, the initial angles are  $q_1(0) = 0[\text{rad}]$  and  $q_2(0) = 1[\text{rad}]$ .

#### A. Simulation Results with Proposed Control Law

The simulation results for the set-point problem are shown in Figs. 7–10. Figs. 7 and 8 depict the joint angles and the trajectory of the arm in the case of  $q_{d1} = \frac{\pi}{2}$  and  $q_{d2} = 0$ , i.e., only shoulder joint is wanted to move. Figs. 9 and 10 describe the joint angles and the trajectory of the arm in the case of  $q_{d1} = 0$  and  $q_{d2} = \frac{\pi}{2}$ , i.e., only elbow joint is wanted to move. Although another joint was moved in both cases, we consider that it is quite natural on human motion.

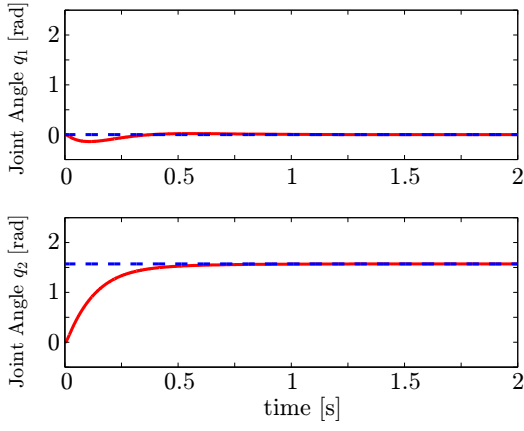


Fig. 9. Step response in the case of  $q_{d1} = 0$ ,  $q_{d2} = \frac{\pi}{2}$ . (solid:Joint angles, dashed:Desired ones).

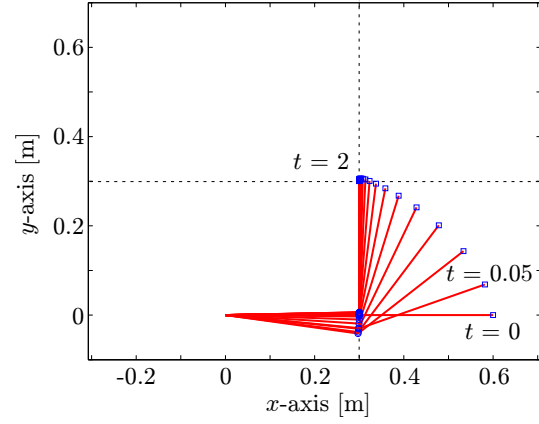


Fig. 10. Trajectory of the arm in the case of  $q_{d1} = 0$ ,  $q_{d2} = \frac{\pi}{2}$ .

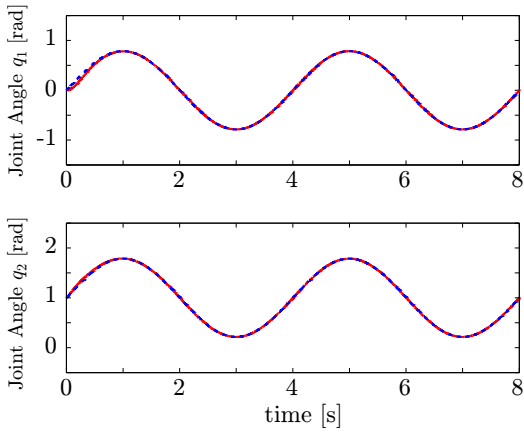


Fig. 11. Trajectory tracking problem ( $\omega = 0.25$ [Hz]) (solid:Joint angles, dashed:Desired ones).

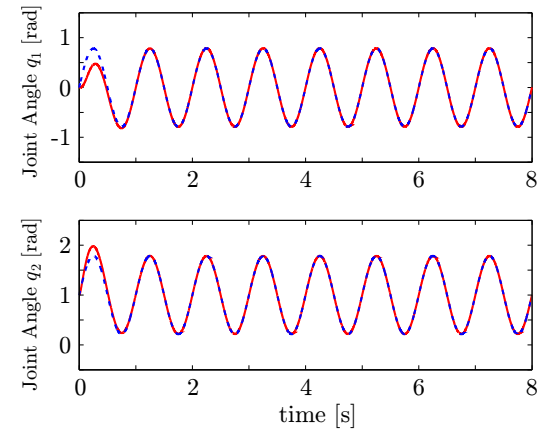


Fig. 12. Trajectory tracking problem ( $\omega = 1$ [Hz]) (solid:Joint angles, dashed:Desired ones).

Specially, it is very difficult to try to move only the elbow joint by oneself.

We give  $q_{d1} = \sin(2\pi\omega t)$  and  $q_{d2} = 1 + \sin(2\pi\omega t)$  as the desired angles for the trajectory tracking problem. Figs. 11 and 12 show the joint angles and desired ones with  $\omega = 0.25$ [Hz] and with  $\omega = 1$ [Hz], respectively. Though both joints have the errors until 0.5[s] in the case of the high frequency, they completely coincide with the desired trajectory after 0.5[s]. From these simulation results, the asymptotic stability can be also confirmed.

### B. Simulation Results with Modified Control Law

In this subsection, we modify the proposed control law (11). Because it is inferred that humans do not measure the joint angles and velocities explicitly, we consider the following sensorless control law

$$\tau = M_b(\theta_d)\ddot{\theta}_d + C_b(\theta_d, \dot{\theta}_d)\dot{\theta}_d + g_b(\theta_d) + K_r\theta_d + B_r\dot{\theta}_d. \quad (17)$$

It is noted that  $\theta$  and  $\dot{\theta}$  are replaced with desired values  $\theta_d$  and  $\dot{\theta}_d$  in Eq. (11), respectively. The block diagram of the modified control law is depicted in Fig. 13. Simulation results

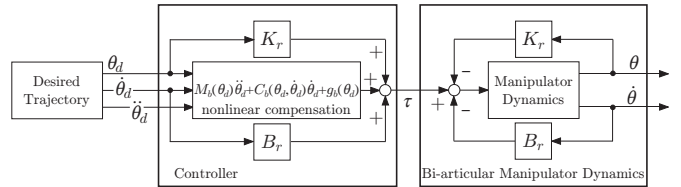


Fig. 13. Block diagram of the modified control law.

by using the modified control law (17) are shown in Figs. 14–17. Although the transient response and the tracking performance are inferior to the proposed control law (11), these simulation results suggest that 2DOF robot manipulators with antagonistic bi-articular muscles could be controlled with a sensorless control law, i.e., the information of joint angles and velocities would not be needed in a control law explicitly. The stability analysis with the sensorless control law has to be discussed in our future work.

## V. CONCLUSIONS

This paper deals with a passivity-based control for 2DOF robot manipulators with antagonistic bi-articular muscles. Stability analysis with respect to our proposed control law,

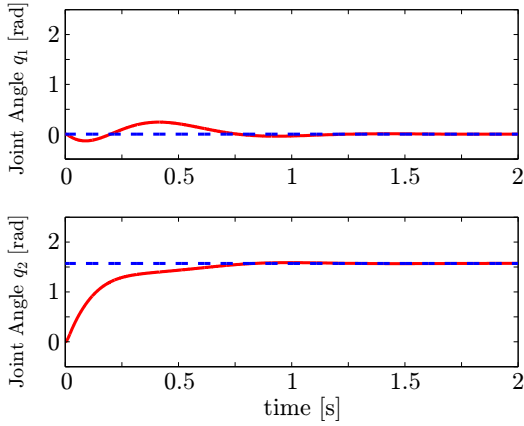


Fig. 14. Step response in the case of  $q_{d1} = 0, q_{d2} = \frac{\pi}{2}$  with a sensorless (solid:Joint angles, dashed:Desired ones).

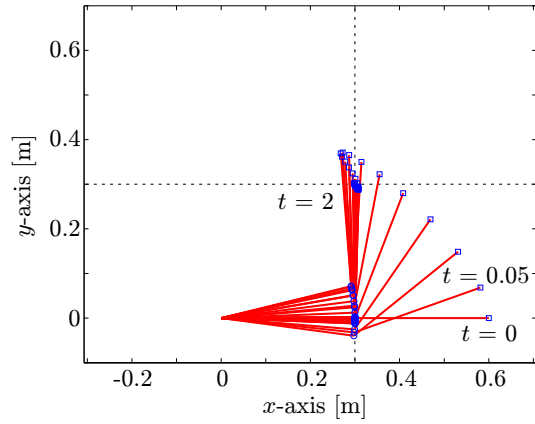


Fig. 15. Trajectory of the arm in the case of  $q_{d1} = 0, q_{d2} = \frac{\pi}{2}$  with a sensorless.

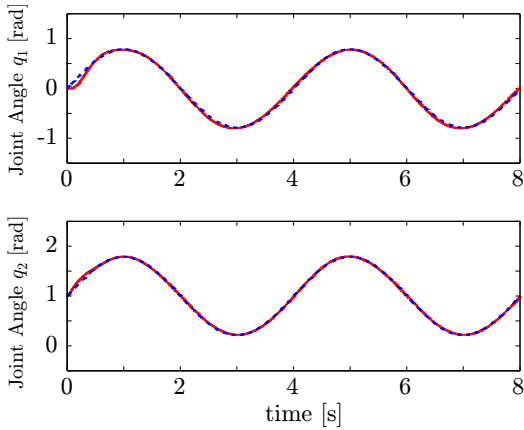


Fig. 16. Trajectory tracking problem with a sensorless( $\omega = 0.25$ [Hz]) (solid:Joint angles, dashed:Desired ones).

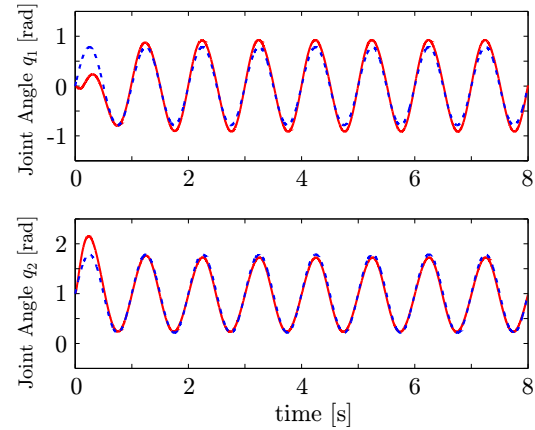


Fig. 17. Trajectory tracking problem with a sensorless( $\omega = 1$ [Hz]) (solid:Joint angles, dashed:Desired ones).

which is one of main contributions of this paper, is discussed by using the important property which is concerned with the passivity, although the passivity of the bi-articular manipulator dynamics can not be shown explicitly. The simulation results show the validity of the proposed method and give the possibility of a sensorless control for 2DOF robot manipulators with antagonistic bi-articular muscles. In our future work, we will discuss the stability analysis with the sensorless control law and integrate the vision based control [2] or vision and force based control [3] in order to consider human motion with five senses.

#### ACKNOWLEDGEMENT

Musculoskeletal Images are from the University of Washington “Musculoskeletal Atlas: A Musculoskeletal Atlas of the Human Body” by Carol Teitz, M.D. and Dan Graney, Ph.D.

#### REFERENCES

- [1] B. Siciliano and O. Khatib (Eds), *Springer Handbook of Robotics*, Springer-Verlag, 2008.
- [2] M. Fujita, H. Kawai and M. W. Spong, “Passivity-based Dynamic Visual Feedback Control for Three Dimensional Target Tracking: Stability and  $L_2$ -gain Performance Analysis,” *IEEE Trans. on Control Systems Technology*, Vol. 15, No. 1, pp. 40–52, 2007.

- [3] H. Kawai, T. Murao and M. Fujita, “Passivity-based Visual Force Feedback Control for Eye-to-Hand Systems,” A. Lazinic and H. Kawai(Eds.), *Robot Manipulators, New Achievements*, IN-TECH, pp. 329-342, 2010.
- [4] E. Guglielmelli, M. J. Johnson and T. Shibata, “Guest Editorial Special Issue on Rehabilitation Robotics,” *IEEE Trans. on Robotics*, Vol. 25, No. 3, pp. 477–480, 2009.
- [5] M. Kuschel, M. Di Luca, M. Buss and R. L. Klatzky, “Combination and Integration in the Perception of Visual-Haptic Compliance Information,” *IEEE Trans. on Haptics*, Vol. 3, No. 4, pp. 234–244, 2010.
- [6] Q. Wang, N. Sharma, M. Johnson and W. E. Dixon, “Adaptive Inverse Optimal Neuromuscular Electrical Stimulation,” *Proc. 2010 IEEE Multi-Conference on Systems and Control*, pp. 1287–1292, 2010.
- [7] M. Kumamoto, T. Oshima and T. Yamamoto, “Control Properties Induced by the Existence of Antagonistic Pairs of Bi-articular Muscles,” *Human Movement Science*, Vol. 13, No. 5, pp. 611–634, 1994.
- [8] M. Kumamoto, *et al.*, *Revolution in Humanoid Robotics*, Tokyo Denki Univ. Press, 2006.
- [9] M. Kumamoto, “Engineering Review of Biological Evolution of Motion Control,” *Proc. of the Int. Symp. on Application of Biomechanical Control Systems to Precision Engineering*, pp. 29–34, 2010.
- [10] S. Oh and Y. Hori, “Development of Two-Degree-of-Freedom Control for Robot Manipulator with Biarticular Muscle Torque,” *Proc. of the 2009 American Control Conference*, pp. 325–330, 2009.
- [11] M. W. Spong and M. Vidyasagar, *Robot Dynamics and Control*, John Wiley & Sons, 1989.
- [12] B. Brogliato, R. Lozano, B. Maschke and O Eglund, *Dissipative Systems Analysis and Control: Theory and Applications (2nd Ed.)*, Springer, 2007.